Vol. 5(1), pp. 1-12, 2026
eISSN: 2976-4009

*ASEAN Journal of Process Control*

*Research Article*

# PI-IMC-Based Controller Design for an Ethanol–Water Distillation Column

**Moo May Yee[1], Gan Jing Wen[1], Chan Ren Yan[1], Noraini Mohd[1]***

[1]School of Energy and Chemical Engineering, Xiamen University Malaysia, Jalan Sunsuria, Bandar Sunsuria, 43900 Sepang, Selangor, MALAYSIA

*Corresponding Author: noraini.mohd@xmu.edu.my

**Abstract:** Distillation column is an important unit operation for multicomponent separation. However, its highly complex and nonlinear characteristics require an effective control strategy to maintain consistent product purity. This work focuses on the design and performance evaluation of an IMC-PI controller for a lab-scale distillation column. A First-Order Plus Dead-Time (FOPDT) model is developed based on experimental data, with model accuracy evaluated using $R^2$ and RMSE values of 0.8857 and 0.0119, respectively. Three PI controller tuning methods; AMIGO, Cohen-Coon, and IMC are applied and assessed based on setpoint and disturbance rejection response using Scilab XCOS simulation. The results show that IMC provides the best balance between overshoot and settling time, with no oscillations occurring. Scilab XCOS simulations are used for tuning and robustness analysis of the IMC PI-controller by introducing variations of the controller time constant, $\tau_c$ and process steady-state gain, $K_p$. Through optimisation and trial-and-error, larger $\tau_c$ results in a more robustly stable controller, slower response with a longer rise time. Among tested values, $\tau_c = 3.25\ min$ demonstrated the best robustness performance, exhibiting only a small overshoot and a short settling time, indicating stable performance under $K_p$ variations. In comparison to the other tuning techniques examined, the suggested IMC–PI controller achieves better setpoint tracking, disturbance rejection, and robustness.

**Keywords:** Controller design, IMC, AMIGO, Cohen-Coon, distillation column, FOPDT, dynamic responses.

## 1. Introduction

In this study, a distillation column was selected for studying dynamic modelling, controller design, simulation, and performance evaluation. Distillation is one of the important separation processes in the chemical industry and was one of our previous laboratories works. A distillation column separates a liquid mixture based on differences in boiling points [1]. In this experiment, a tray distillation column was used to separate a binary mixture of ethanol and water, where vapor-liquid equilibrium is established on each tray. Figure 1 shown the tray distillation column. When heat is supplied, the more volatile component (ethanol) vaporizes first, travelling up through the column and condenses in the condenser as top product, while the less volatile component remains mostly in the liquid phase and is collected as bottom product [2].

The distillation column is known to be a highly complex and nonlinear process because it involves dual composition control of high purity distillation process [2]. In a distillation column, parameter uncertainty arises from measuring values due to the unknown system parameters, such as

friction and mass coefficient [3]. In addition, distillation often exhibits a time delay, which refers to the period between a change in process input and the observable response of the process output [4]. The time delay in the distillation process can result from liquid hold-up in the column, which affects the mass and heat transfer and consequently the whole dynamic response of the system [5].

Furthermore, distillation columns are costly to operate and energy intensive because substantial energy is required to drive the separation process [6]. A poor control system may lead to unstable operation, increase energy consumption and operation cost. Therefore, an effective process control system is important for maintaining stable operating conditions and supporting energy efficient operation.

This study evaluates PI controller model-based design for a laboratory-scale ethanol-water distillation column. The experimental data collected are used to develop a First-Order Plus Dead-Time (FOPDT) model. Based on this model, simulation and performance evaluation were conducted to enhance process utilization using Scilab simulations. Controller design was developed using three methods: PI-Cohen-Coon, PI-IMC, and PI-AMIGO. Each PI controller was evaluated under set-point and disturbance changes. The performance of each method was analyzed, and the best-performing method was selected through optimization and tuning, followed by a robustness analysis.

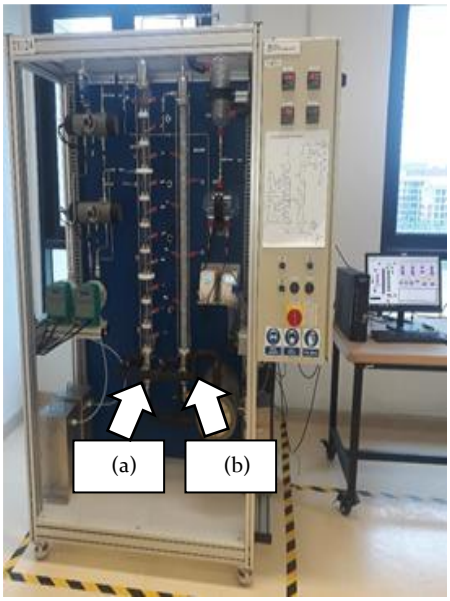



Figure 1. Distillation columns. (a): Tray column (used in this study), (b): Packed column.

## 2. Materials and Methods

### *2.1. Assumption and simplification*

This study adopted several assumptions to simplify the dynamic analysis and controller design of the distillation column. Based on the literature [7], experimental data obtained from several runs with sufficiently long observation times indicated that the dynamic behavior of the ethanol-water distillation system could be reasonably approximated as a First Order Plus Delay Time (FOPDT) model. Therefore, the FOPDT model was adopted in this study to represent the dynamic behavior. In addition, a process time delay of 2.25 min was adopted from the same literature due to the unavailability of precise time delay data for the laboratory-scale distillation column used in this study [7]. For process analysis and controller design, the reflux ratio was selected as the manipulated variable (MV), while the mole fraction of ethanol in the top product was selected as the controlled variable (CV). Furthermore, feed composition was considered as the main disturbance variable (DV) affecting the system dynamics. The feed flow rate, condenser temperature and reboiler temperature were assumed to remain constant throughout the experiment to reduce system complexity and simplify the analysis.

### *2.2. Transfer Function Development*

A FOPDT model was developed based on the experimental results. The transfer function describes the behaviour of the system and how the input influences the output [8]. The steady state

gain, K, represents the ratio of the change in output to the change in input at steady state. The time constant, τ, describes how quickly the system responds to the input change, while the time delay, θ represents the time before the output begins to respond. The process can be approximated using the FOPDT structure given by:

$$G(s) = \frac{Ke^{-\theta s}}{\tau s + 1} \quad (1)$$

In this study, the values of K and τ values were determined from the empirical data as 0.0642 and 26.94 min, respectively. The time delay was taken as 2.25 min [7]. The ethanol mole fraction was recorded until the system reached steady state, increasing from 0.6854 at the start of the experiment to 0.8031 at 60 min, while a step change from 0 to 1.8333 of reflux ratio was introduced to the system, and was kept constant at 1.8333 throughout the experiment. Using the values of K, τ and θ, the transfer function was developed as shown below:

$$G(s) = \frac{0.0642e^{-2.25s}}{26.94s + 1} \quad (2)$$

*2.3. Model Validation*

For the model validation, a step input of 1.8333 of reflux ratio was introduced into the distillation column system. The Laplace transform was applied to obtain a linearized model. The experimental data were obtained directly from the experiment, while the model response data were calculated using the developed transfer function, with a detailed sample calculation shown in the appendix. Figure 2 illustrates the profiles of both the experimental and FOPDT model, which were used to analyse the model mismatch and evaluate how well the developed model fits the experimental data.

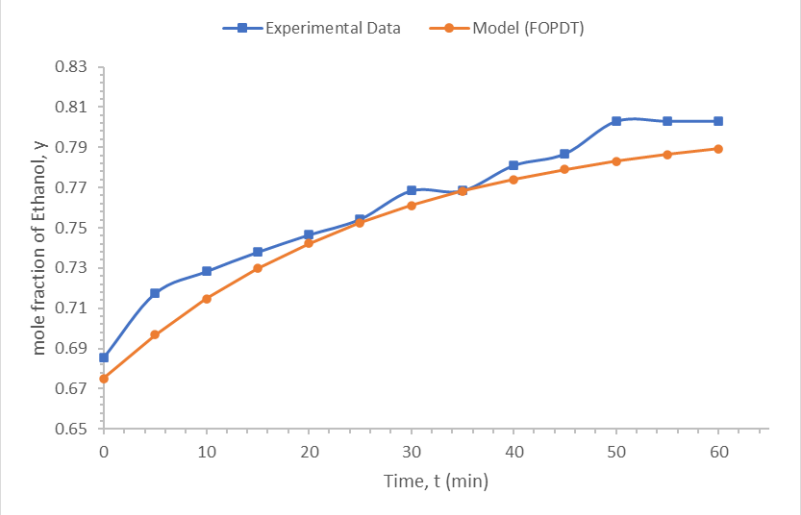



Figure 2. Comparison of ethanol mole fraction over time between experimental data and the FOPDT model.

Figure 2 shows that both experimental and model responses show a similar increasing trend, indicating that the FOPDT model fit well with the experimental data and successfully predicts the system behaviour. However, the ethanol mole fraction obtained from the model is consistently lower than the experimental data over time. This discrepancy may be attributed to the simplification of the actual distillation process into a FOPDT model, which may not fully predict the non-linear vapor-liquid equilibrium behaviour in the distillation process. To further evaluated how well the model fits the experimental data, the discrepancy between the generated model and the actual data was evaluated using the root mean squared error (RMSE) index and the $R^2$ value. The formula for calculating $R^2$ as shown in *Equation 3* [9], while the formula to calculate RMSE is shown in *Equation 4* [10].

Determination of $R^2$:

$$R^2 = 1 - \frac{\sum_{i=1}^{n}(y_i - \hat{y}_i)^2}{\sum_{i=1}^{n}(y_i - \bar{y}_i)^2} \quad (3)$$

Determination of RMSE:

$$RMSE = \sqrt{\frac{\sum_{i=1}^{n}(y_i - \hat{y}_i)^2}{n}} \quad (4)$$

where $y_i$ and $\hat{y}_i$ are the experimental and model-predicted data at the time $t_i$, while $\overline{y}_i$ is the mean experimental data ($y$) and $n$ is the total number of data points.

An $R^2$ of 1 and an RMSE of 0 indicates a perfectly fitted model with experimental data, meaning the transfer function accurately represents the data [10]. In this study, the developed transfer function obtained a $R^2$ value of 0.8857 (close to 1) and RMSE of 0.0119 (close to 0), confirming strong agreement with the experimental response. Additionally, since this study assumes an FOPDT system, the high $R^2$ and low RMSE values demonstrate that the FOPTD transfer function is reliable for controller design and analysis.

### *2.4. Dynamic Behavior*

In this study, the process exhibits a time delay of 2.25 $min$, meaning the output starts to respond 2.25 minutes after a control is applied [11]. Time delay commonly occurs due to transport delays between the actuators and sensor, sensor processing time, and actuator reaction time [12]. Besides that, the small $K_C$ of 0.0642 in this process indicates low sensitivity, meaning the output responds slowly and slightly to input changes, resulting in a stable but sluggish system performance [13].

For a closed-loop system, the settling time is approximately $5\tau$ to reach the final state value [14]. Thus, the system requires about 134.7 $min$ to reach a steady state, confirming that the process responds slowly and takes a long time to settle. The process is also considered a lag dominant process as the $\frac{\tau}{\theta}$ ratio is calculated to be 11.9733, which exceeds 4. $\frac{\tau}{\theta}$ ratio exceeding 4 indicates the system is easier to control and perform well, making PID control effective for this type of process [15].

The dynamic behaviour of a transfer function model can be characterized by the locations of its poles and zeros [14]. Poles and zeros are the roots of the denominator and numerator polynomials of the transfer function, respectively. Poles and zeros calculations are shown in the appendix. In this study, the system has a pole of $-0.0371$ located in the left half plane (LHP) with s < 0 at denominator, indicating a stable system [16]. The zero is 0.4444 is in the right half plane (RHP) with s > 0 at numerical. These zero results from the Taylor series approximation of the time delay and does not affect system stability but can cause an inverse response to a step change in the input, reflecting the effect of the time delay on the system's response [14,17].

### *2.5. Stability Analysis*

For the stability analysis, a proportional (P) controller was used, and the characteristic equation is presented in *Equation 5*. By substituting $G_{OL} = G_v G_p G_c G_m$ into Equation 5, as shown in *Equation 6*, where $G_p = \frac{0.0642e^{-2.25s}}{26.94s+1}$, $G_c = K_c$ and $G_v = G_m = 1$. Thus, the stability range of $K_C$ can be determined, as shown in *Equation 6*, by Pade approximation and the Routh array criterion. The detailed calculations are shown in the appendix. The characteristic equation for a closed-loop system:

$$G_{OL} + 1 = 0 \tag{5}$$

Simplified characteristic equation:

$$30.3075s^2 + (28.0650 - 0.0722K_C)s + 0.0642K_C + 1 = 0 \tag{6}$$

Stability Range of $K_C$:

$$-15.5763 < K_C < 388.7119$$

The system is stable when $K_C$ ranges from $-15.5763$ to $388.7119$. This stability limit was determined based on the P controller only. However, if P controller remains stable within this range, the PI and PID controllers will also be stable within the same $K_C$ range. Thus, this stability ranges of $K_C$ can be applied to all three controller types for further controller design in this study.

### *2.6. PI Controller Design (SISO)*

PI control is one of the most commonly application in industry due to its simple structure, good robustness and wide application range. In this study, PI control was selected because the integral (I) action eliminates steady state error while avoiding the added complexity of derivative (D) action [14]. This provides a suitable balance between control performance and robustness while maintaining a simple controller structure. Besides, PI controller tuning method are commonly developed based on proves models, especially for FOPDT model. Thus, it is essential to tune the controller to get the optimal values of $K_C$ and $\tau_I$ to achieve the desired performance parameter, such as system overshoot, rise time and

settling time [18]. In this paper, the PI tuning method were used based on Cohen-Coon, Approximate M-constrained Integral Gain Optimisation (AMIGO), and Internal model control (IMC) methods. All three methods are model-based with controller parameters derived from the FOPDT function developed in Section 2.2.

The Cohen-Coon tuning method is primarily applied to single-order systems with clearly identifiable mathematical models, especially plants that exhibit noticeable dead-time characteristics [19]. This method provides explicit formulas for calculating the PI controller parameters, namely the controller gains $K_C$ and the integral time $\tau_I$. The procedure for determining these parameters using the Cohen-Coon method is shown below:

$$K_C = \frac{1}{K_P}\frac{\tau_P}{\theta_P}\left(\frac{9}{10} + \frac{\theta_P}{12\tau_P}\right) \tag{7}$$

$$\tau_I = \theta_P\left(\frac{30 + 3\frac{\theta_P}{\tau_P}}{9 + 20\frac{\theta_P}{\tau_P}}\right) \tag{8}$$

The AMIGO tuning rules were selected as a point of comparison because they provide controllers with good performance and robustness characteristics [20]. Moreover, AMIGO supports general nonlinear dynamic models through a simple and flexible tuning framework [21]. The AMIGO tuning approach is based on the 63% step response experiment, where model parameters are identified from the process reaction curve. The primary design objective is to minimize the integrated error (IE) resulting from the load disturbances while satisfying specified robustness constraints. The corresponding tuning rules are given as follows:

$$K = \frac{1}{K_P}\left(0.15 + 0.35\frac{T}{L} - \frac{T^2}{(L+T)^2}\right) \tag{9}$$

$$T_i = 0.35L + \frac{13LT^2}{T^2 + 12LT + 7L^2} \tag{10}$$

where T represents the time constant, and L is the time delay.

Moreover, the IMC approach incorporates the process model into the controller structure, enabling the development of a control system that is both stable and robust [22]. A stable control system maintains appropriate control actions in response to dynamic changes within the process. One of the key advantages of the IMC approach is that it explicitly accounts for model uncertainty and facilitates a systematic trade-off between control performance and robustness [23]. The corresponding tuning rules are given as follows:

$$K_C = \frac{1}{K_P}\left(\frac{\tau}{\tau_c + \theta}\right) \tag{11}$$

$$\tau_I = \tau \tag{12}$$

*2.7. Methodology*

The methodology adopted in this study involved process identification, identification of CV, MV and DV, development of the transfer function model, controller selection and tuning, and evaluation of controller performance through setpoint and disturbance change. The reflux ratio was selected as the manipulated variable (input), while the ethanol mole fraction in the top product was the controlled variable (output). A constant reflux ratio of 1.8333 was applied to achieve a high distillate purity. Top product samples were collected at 5-minute intervals to obtain the system's response for transfer function identification, as described in Section 2.3.

## 3. Results and Discussion

The three tuning methods, such as Cohen-Coon, IMC, and AMIGO, were applied to control the ethanol mole fraction in distillate and evaluate the system's response under setpoint changes and disturbance conditions. For computational simplicity and in accordance with industry practice, the scaled ethanol mole fraction in the distillate is represented by the setpoints of 90, 180, and 270 used in the setpoint changes and disturbance rejection test in section 3.1.1. Accordingly, PI controllers were designed using parameters obtained from each of these methods. *Table 1.* presents the calculated tuning parameters.

Table 1. PI controller parameters for Cohen-Coon, IMC, and AMIGO methods.

| | Cohen-Coon | IMC | AMIGO |
|---|---|---|---|
| **P** | 54.344 | 93.2503 | 169.1485 |
| **I** | 3.6113 | 3.4614 | 26.5173 |

### *3.1. Simulation and Performance Evaluation*

The simulation and performance evaluation were divided into three main sections. Section 3.1.1 involved determining the controller responses for both setpoint tracking and disturbance rejection scenarios using all three tuning methods. Section 3.1.2 focused specifically on tuning and robustness analysis based on the best method proposed in the first section. Section 3.1.3 discussed the limitations of the current study and the corresponding recommendations for future work. This three-part evaluation framework was used to systematically compare the methods, select the single best-performing tuning approach for the system, and identify directions for further improvement.

#### 3.1.1. *Simulation for Setpoint and Disturbance Changes*

For a well-designed controlled system, the output response should be smooth and stable, with minimal or no oscillations when subjected to changes in the setpoint or external disturbances. Subsequently, simulations were carried out using Scilab, as illustrated in Figure 3. The simulations employ the designed PI controllers to examine system performance under both setpoint changes and disturbance rejection for the three tuning methods.

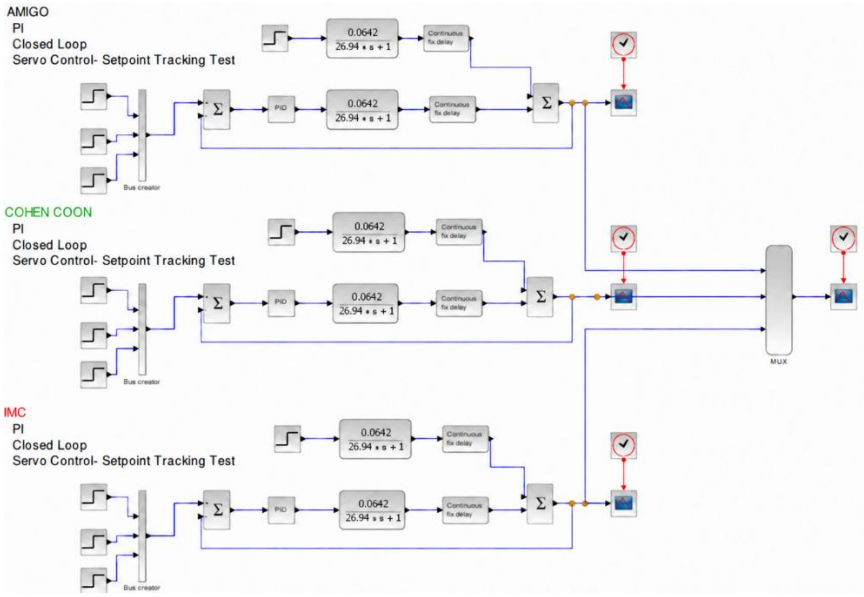



Figure 3. Simulation of setpoint tracking and disturbance rejection tests using Scilab.

#### 3.1.1.1. *Setpoint Change*

Figure 4 illustrates the system's output response to step changes in the setpoint. The setpoint is adjusted sequentially from 0 to 90, then 90 to 180, and finally to 270. All three controllers reached their respective target values, indicating successful setpoint tracking. To further evaluate controller performance, the dynamic behaviour of the underdamped process is assessed using six standard performance criteria, which are overshoot, settling time, rise time, time to first peak, decay ratio, and period of oscillation, as summarized in *Table 2*.

From *Table 2*, the Cohen-coon method exhibited significant overshoot across all setpoint changes and produced significant oscillations. In contrast, the IMC method showed the lowest overshoot, indicating lower risk of instability in the control system.

The IMC method also demonstrated the shortest settling time, where it shows a faster response and better performance due to the reduced duration of deviation from the desired setpoint. On the other hand, the Cohen-Coon method exhibited a slightly longer settling time than the AMIGO method, this suggested that both require more gradual adjustments to reach the new steady-state conditions. This demonstrated a comparatively slower convergence to the target operating point.

Moreover, by comparing the rise time, Cohen-Coon method achieved the shortest rise time, where this showed a faster response. However, this fast response comes at the expense of stability, as it introduces a high percentage of overshoot. The IMC method exhibits a moderate rise time, while the AMIGO method showed the longest rise time, indicating the slowest response among the three methods.

A similar trend was observed for the time to first peak. The Cohen-Coon method has the shortest peak time, meaning it reached the maximum value most quickly, followed by the IMC method and then the AMIGO method. Despite its fast peak response, the Cohen-Coon method suffered from the oscillatory behaviour, whereas both IMC and AMIGO demonstrated stable response without noticeable oscillations.

Furthermore, only the Cohen-Coon method exhibited measurable decay ratio and oscillation period across different setpoints as oscillations result in the appearance of the second peak. This indicated an underdamped and less stable response compared to the other methods. Overall, the IMC method demonstrated the best performance. It achieved minimal overshoot with moderate settling, rise, and peak times under varying setpoint changes. Collectively, these characteristics allow the IMC controller to return to the setpoint and steady state more efficiently than the other tuning methods.

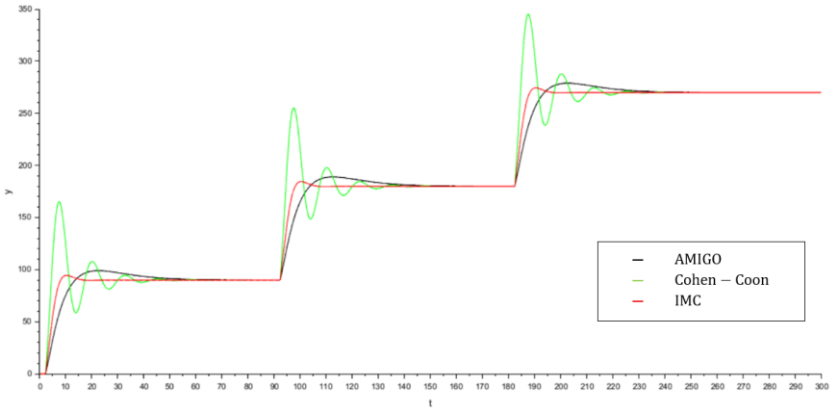



Figure 4. Simulation results of setpoint tracking at $y_{sp}$ = 90, 180, 270 using Cohen-Coon, IMC, and AMIGO tuning methods.

Table 2. Performance Criteria for three different setpoints of $y_{sp}$ = 90, 180, 270 using different methods.

| **$y_{sp}$ = 90** | | | |
|---|---|---|---|
| **Performance Criteria** | **Cohen-Coon** | **IMC** | **AMIGO** |
| **Overshoot (%)** | 83.56 | 4.05 | 9.90 |
| **Settling time, $t_s$ (min)** | 33.853 | 12.570 | 27.405 |
| **Rise time, $t_r$ (min)** | 4.449 | 8.416 | 13.614 |
| **Time to first peak, $t_p$ (min)** | 7.401 | 10.67 | 22.393 |
| **Decay ratio, DR** | 0.2373 | - | - |
| **Period of Oscillation, P (min)** | 12.705 | - | - |
| **$y_{sp}$ = 180** | | | |
| **Overshoot (%)** | 83.60 | 4.04 | 9.90 |
| **Settling time, $t_s$ (min)** | 28.288 | 12.570 | 27.393 |
| **Rise time, $t_r$ (min)** | 4.45 | 8.416 | 13.623 |
| **Time to first peak, $t_p$ (min)** | 7.4 | 10.643 | 22.591 |
| **Decay ratio, DR** | 0.2375 | - | - |
| **Period of Oscillation, P (min)** | 12.698 | - | - |
| **$y_{sp}$ = 270** | | | |
| **Overshoot (%)** | 83.60 | 4.05 | 9.90 |
| **Settling time, $t_s$ (min)** | 27.873 | 12.57 | 27.405 |
| **Rise time, $t_r$ (min)** | 4.449 | 8.417 | 13.615 |
| **Time to first peak, $t_p$ (min)** | 7.399 | 10.678 | 22.389 |
| **Decay ratio, DR** | 0.2375 | - | - |
| **Period of Oscillation, P (min)** | 12.701 | - | - |

3.1.1.2. *Disturbance rejection performance of the flow control system*

Some systems require a strong capability to maintain stability against high-frequency external disturbances rather than responding primarily to set-point changes. This specifically referred to systems that are affected by noise or external interference. A properly tuned control system should therefore provide a reasonably damped response with minimum overshoot and fast recovery to the setpoint when disturbances are imposed. The main disturbance rejection performance objectives are the minimization of peak error and the integrated absolute error (IAE). Disturbance tends to push the process (controlled variable) away from the desired setpoint [24]. Under such conditions, accurate setpoint tracking becomes difficult. Hence, a controller is considered effective if it can reject disturbance, as this capability directly contributes to the overall stability of the control system.

In this study, disturbance tests were conducted with a setpoint change at 250 and a final value of 300. Figure 5 illustrates the response of all PI controllers, where the red circled region highlights the disturbance more clearly. From the results, only small deviations due to disturbance are observed for all three turning methods, this shows satisfactory disturbance rejection performance. *Table 3* presents a summary of the performance criteria for the three tuning methods.

Based on the disturbance rejection test, the IMC methods demonstrate the best overall performance, as it achieves a balanced compromise between overshoot, settling time, and no oscillations occurred. Although the Cohen-Coon method exhibits the lowest overshoot and the shortest disturbance rejection time, but it suffers from oscillatory behaviour, which is undesirable for stable control performance because it amplifies noise and may lead to instability. In contrast, AMIGO method results in the highest overshoot and longest settling time, indicating weaker disturbance rejection. Therefore, the IMC method is selected for further tuning and robustness analysis as it provides superior overall performance compared to the other methods.

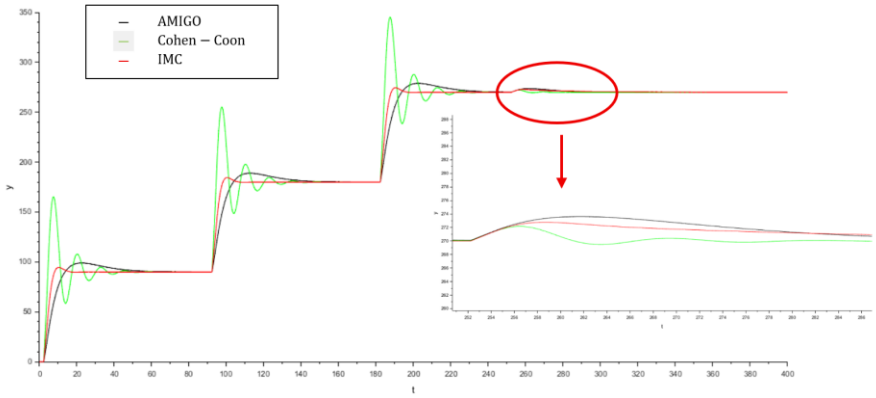



Figure 5. Simulation results of disturbance rejection test at $y_{sp}$ = 270 using Cohen-Coon, IMC, and AMIGO methods.

Table 3. Performance criteria in disturbance rejection for Cohen-Coon, IMC, and AMIGO methods at the setpoint, $y_{sp}$ = 270.

| **$y_{sp}$ = 270** | | | |
|---|---|---|---|
| **Performance Criteria** | **Cohen-Coon** | **IMC** | **AMIGO** |
| **Maximum disturbance error (%)** | 0.80 | 1.04 | 1.34 |
| **Settling time, $t_s$ (min)** | 79.146 | 89.883 | 90.580 |
| **Period of Oscillation, P (min)** | 12.925 | - | - |

3.1.2. *Simulation of Tuning and Robustness*

3.1.2.1. *Tuning Analysis*

This tuning analysis is implemented to evaluate the sensitivity of the designed controller IMC to variations in its controller time constant, $\tau_c$ by increasing it from 2.25 to 3.25 and 5 min, and decreasing it to 1.25 min. Figure 6 shows the responses of system to $\tau_c$ change for IMC. Table 4 shows the summary of performance criteria for IMC controller tuning and robustness analysis. The results showed that when the $\tau_c$ was reduced from 2.25 to 1.25 min, resulting in faster response time, as the rise time decreased from 8.417 to 6.130 min, but oscillation and overshoot were observed at $\tau_c$ = 1.25 min. This indicates that when

$\tau_c$ decreases, the controller more aggressive and stability of the system reduces as reflected by the increase in settling time, $t_s$ from 10.970 to 11.446 min when the $\tau_c$ decreased from 2.25 to 1.25 min. Conversely, increasing $\tau_c$ from 2.25 to 3.25 min, the response time became slower as the rise time increased from 8.417 to 14.681. Further increasing $\tau_c$ to 5 min made the response time became even more slower as the rise time was increased significantly to 46.232 min. However, no overshoot and oscillation occurred when $\tau_c$ increased to 3.25 and 5 min. This indicates the system is capable of maintaining stable under these tuning settings, although the response becomes slower to reach the setpoint. This can be explained by the performance-robustness (stability) trade-off for IMC-PI/PID controller. A larger closed-loop time constant results in a more robustly stable controller that produces a slower response with a longer rise time, and vice versa [25]. In short, $\tau_c$ = 3.25 min provides the best controller performance, as the system remains stable with no oscillation or overshoot, even though the response is slightly slower compared to smaller $\tau_c$ values.

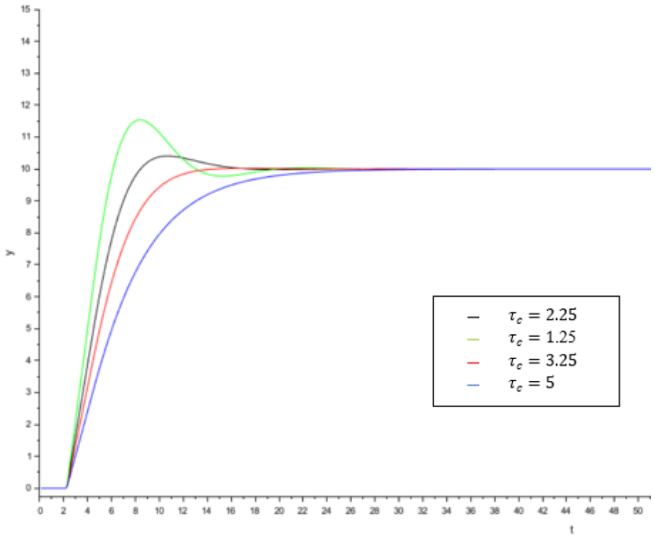
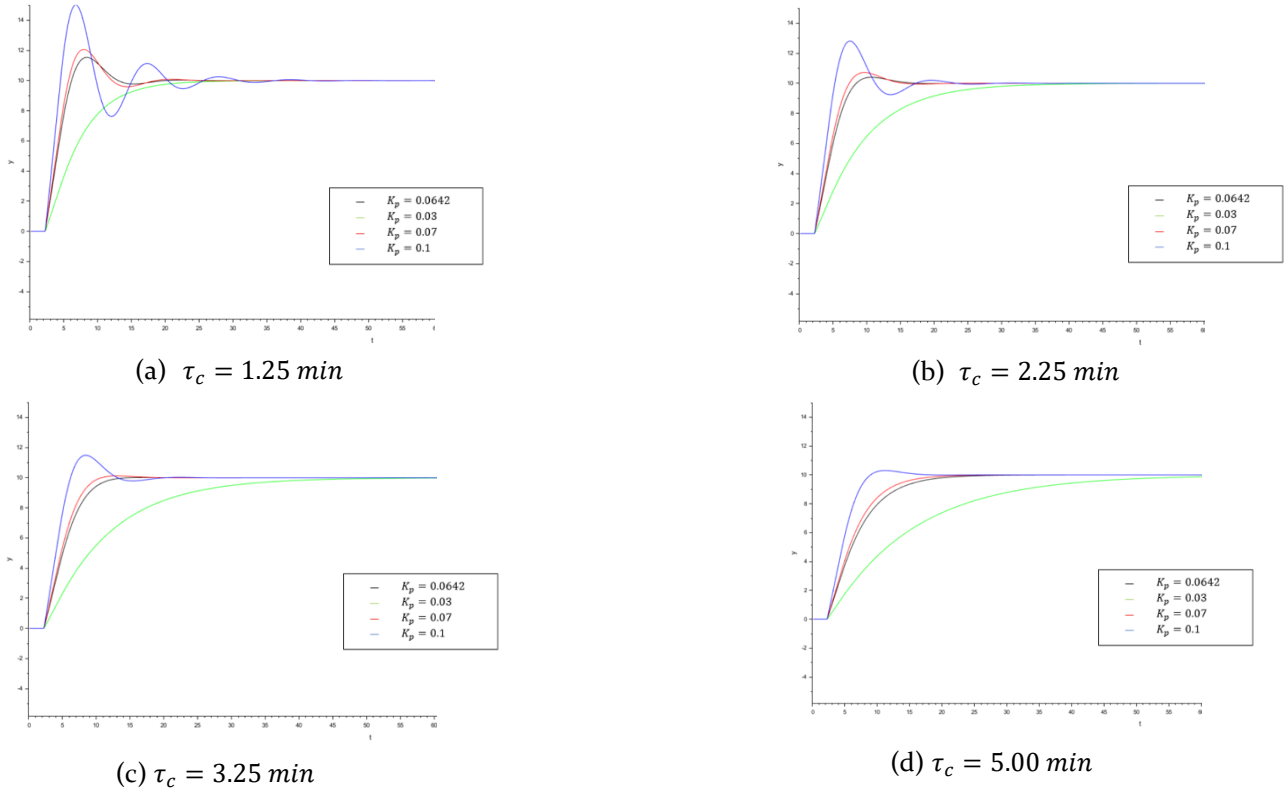



Figure 6. Responses of system to $\tau_c$ change for IMC.

3.1.2.2. *Robustness Analysis*

The concept of "robustness" refers to maintaining numerous systems features as possible in the face of uncertainties in the plant and controller model or signals [26]. More precisely, if the plant or controller has uncertainties (and/or unmodeled dynamics) or there is disturbance and noise infiltration, it is desired to maintain stability and even performance specifications [26]. Therefore, robust performance can be utilised to determine the stability of the system. In this work, the process steady state gain, $K_p$ was varied by increasing it from 0.0642 to 0.07 and 0.1, and decreasing it to 0.03, to evaluate the robustness of the system for each previously selected $\tau_c$ value. Figure 7 shows the performance of robustness for different $K_p$ and $\tau_c$ values. Based on the Figure 7, it can be observed that as the $\tau_c$ increases, the response curve become flatter and more stable system across all $K_p$ values. The results suggested that a slower response time and the increase in $t_s$ and showed improved robustness of the system. These findings are consistent with the tuning analysis, which showed that the higher the $\tau_c$ values result in slower response time with more robustly stable controller. Based on Figure 7*(a),* the system shows the poorest stability at $\tau_c = 1.25\ min$, as the response exhibits severe oscillations and overshoot, especially when $K_p$ = 0.1000. By increasing the $\tau_c$ to 2.25 min, as shown in Figure 7 *(b)* the oscillations are still present but the overshoot is significantly reduced compared to $\tau_c = 1.25\ min$. At $\tau_c = 5\ min$, Figure 7*(d)* shows that no oscillation and overshoot occur for any $K_p$ value, but the time required to reach steady-state is much longer for each $K_p$ values compared to smaller $\tau_c$. On the other hand, Figure 7*(c)* and *Table 4* demonstrate that $\tau_c = 3.25\ min$ provides an optimal performance, with only one overshoot was observed at $K_p$ = 0.1000 with a value of 3.03 %, while all other $K_p$ show no oscillatory and overshoot. This demonstrated that the $\tau_c = 3.25\ min$ made the system remains stable across $K_p$ variations Therefore, $\tau_c = 3.25\ min$ shows the best robustness performance among all $\tau_c$ . Although a small overshoot occurs at $K_p$ = 0.1000, but the $t_s$ remains short, indicating the system can quickly return to setpoint value and maintain stability under $K_p$ variations.




(a) $\tau_c = 1.25\ min$ (b) $\tau_c = 2.25\ min$

(c) $\tau_c = 3.25\ min$ (d) $\tau_c = 5.00\ min$

Figure 7. Robustness performance in different $K_p$ and $\tau_c$ values (a) $\tau_c = 1.25\ min$; (b) $\tau_c = 2.25\ min$; (c) $\tau_c = 3.25\ min$; (d) $\tau_c = 5.00\ min$.

Table 4. Summary performance criteria for IMC controller tuning and robustness analysis.

| **Tuning** | | | | |
|---|---|---|---|---|
| **$\tau_c$ (min)** | **1.25** | **2.25** | **3.25** | **5.00** |
| **Overshoot (%)** | 15.370 | 7.000 | - | - |
| **Settling time, $t_s$ (min)** | 11.446 | 10.970 | 10.226 | 16.051 |
| **Rise time, $t_r$ (min)** | 6.130 | 8.417 | 14.681 | 46.323 |
| **Time to first peak, $t_p$ (min)** | 8.400 | 10.700 | - | - |
| **Decay ratio, DR** | 0.022 | - | - | - |
| **Period of Oscillation, P (min)** | 13.758 | - | - | - |
| **Robustness ($\tau_c = 3.25\ min$)** | | | | |
| **$K_p$** | **0.0300** | **0.0642** | **0.0700** | **0.1000** |
| **Overshoot (%)** | - | - | - | 3.030 |
| **Settling time, $t_s$ (min)** | 41.630 | 16.065 | 14.050 | 11.956 |
| **Rise time, $t_r$ (min)** | 132.232 | 45.909 | 38.402 | 8.952 |
| **Time to first peak, $t_p$ (min)** | - | - | - | 11.249 |
| **Decay ratio, DR** | - | - | - | - |
| **Period of Oscillation, P (min)** | - | - | - | - |

3.1.3. *Limitations and Future Work*

The IMC-PI controller with $\tau_c = 3.25\ min$ demonstrated the best robustness and stable control performance for the distillation process. However, several limitations should be considered when analyzing the results. First, the process time delay of 2.25 *min* was obtained from literature rather than determined directly from the experimental data. This estimated value may introduce discrepancies between the developed model and the actual dynamic behaviour of the distillation process. Therefore, the actual process time delay should be experimentally determined in future studies using a precise data acquisition system, such as a SIMEX recorder, to record the process data at finer time intervals and improve the accuracy of time delay estimation. Furthermore, only a single step change in the reflux ratio was applied, which limited the assessment of system responses and controller performance under

different operating conditions. This may restrict the ability to fully capture system behavior, representing a limitation of the developed model in this study. Future studies should therefore apply step changes of varying magnitudes in the reflux ratio to further validate the model and evaluate controller performance.

## 4. Conclusions

In conclusion, the transfer function of the lab-scale distillation column was developed using experimental data and is expressed as $G(s) = \frac{0.0642e^{-2.25s}}{26.94s+1}$. PI controller tuning was performed using Cohen-Coon, IMC, and AMIGO methods to determine stability and performance of the system. The IMC PI-controller with P=93.2503 and I=3.4614 was selected as the best performing method. This is because it achieved a balanced compromise between maximum disturbance error of 1.04 % and settling time of 89.883 min, and no oscillations occurred in disturbance rejection test at $y_{sp}$ = 270. Besides, tuning analysis was performed for the best IMC PI-controller method, showing that high $\tau_c$ values, result in a more robustly stable controller, but slower response with a longer rise time. Among variations of $\tau_c$ values, $\tau_c$ = 3.25 min provided the best controller performance, maintaining system stability without oscillation or overshoot. Additionally, $\tau_c = 3.25\ min$ also shows the best robustness performance, producing optimal performance with short settling time, no oscillations, only one minor overshoot of 3.03 % at $K_p$ = 0.1000, indicating stable performance under $K_p$ variations. To further improve model accuracy and enhance the applicability of the developed controller, future work should experimentally determine the actual process time delay and assess controller performance using analysis of IAE, ISE, or RMSE. In addition, step changes of different magnitudes in the reflux ratio should be investigated to further validate the dynamic model and evaluate controller performance over a wider range of operating conditions.

**Acknowledgments:** The authors would like to thank to School of Engineering and Chemical Engineering, Xiamen University Malaysia that has provided the access to the laboratory-scale distillation column. The authors also wish to thank Assistant Professor Ts. Dr. Noraini binti Mohd and lab officers for their guidance and support throughout this project. We greatly acknowledge the financial support from the XMUM Research Fund (XMUMRF/2025-C15/IENG/0079).

## References

1. Stichlmair, J.; Klein, H.; Rehfeldt, S. Distillation. 2021. https://doi.org/10.1002/9781119414674.
2. Diaz, S.; Perez-Correa, J. R.; Cipriano, A.; Fernandez-Fernandez, M. Intelligent Control Applications on a Binary Distillation Column. 2016 IEEE International Conference on Automatica (ICA-ACCA) 2016, 1–8. https://doi.org/10.1109/ica-acca.2016.7778496.
3. Biswas, P. P.; Ray, S.; Samanta, A. N. Nonlinear Control of High Purity Distillation Column under Input Saturation and Parametric Uncertainty. Journal of Process Control 2009, 19 (1), 75–84. https://doi.org/10.1016/j.jprocont.2008.01.007.
4. Al Kalbani, F.; Zhang, J. Inferential Composition Control of a Distillation Column Using Active Disturbance Rejection Control with Soft Sensors. Sensors 2023, 23 (2), 1019. https://doi.org/10.3390/s23021019.
5. Zhang, X.; Zhang, W.; Jian, C.; Zhang, J. Role of Holdup in Batch Distillation. Huagong Xuebao/Journal of Chemical Industry and Engineering (China) 2004, 55 (11), 1827–1832.
6. Sivieri, F. M.; Teixeira, E. P. Identification of the Dynamic Model of a Distillation Column. International Journal of Advanced Engineering Research and Science 2019, 6 (6), 466–470. https://doi.org/10.22161/ijaers.6.6.47.
7. Rohman, A. S.; Rusmin, P. H.; Maulidda, R.; Idris Hidayat, E. M.; Machbub, C.; Mahayana, D. Modelling of the Mini Batch Distillation Column. International Journal on Electrical Engineering and Informatics 2018, 10 (2), 350–368. https://doi.org/10.15676/ijeei.2018.10.2.11.
8. Yang, X.-S. Laplace Transforms. Elsevier eBooks 2017, 187–198. https://doi.org/10.1016/b978-0-12-809730-4.00022-7.

9. Mohammad, N. N.; Muhamad; Mohd; Najidah Hambali. Reformulated Tangent Method Application in PID Tuning for Controllability of Agarwood Hydro Distillation Pot. Journal of Electrical & Electronic Systems Research 2025, 26 (APR2025), 88–95. https://doi.org/10.24191/jeesr.v26i1.011.
10. Holden, N. M.; Wolfe, M. L.; Ogejo, J. A.; Enda John Cummins; American. Introduction to Biosystems Engineering; American Society Of Agricultural And Biological Engineers ; Blacksburg, Va: St Joseph, Mi, 2020.
11. Staff, C. E. How to handle the deadtime that hampers process control - Control Engineering. Control Engineering. https://www.controleng.com/deadtime-hampers-process-control/.
12. Normey-Rico, J. E.; Santos; Rodolfo; Torrico, B. C. Control of Dead-Time Process: From the Smith Predictor to General Multi-Input Multi-Output Dead-Time Compensators. Frontiers in control engineering 2022, 3. https://doi.org/10.3389/fcteg.2022.953768.
13. C Shreesha; Gudi, R. D. Control-relevant Identification with Steady State Gain Matching. https://www.researchgate.net/publication/265097285_Control-relevant_Identification_with_Steady_State_Gain_Matching.
14. Seborg, D. E.; Edgar, T. F.; Mellichamp, D. A.; Doyle, F. J. Process Dynamics and Control, 4th ed.; Wiley: Hoboken, Nj, 2017.
15. Bullerdiek, E. PID spotlight, part 6: Deadtime? How to boost controller performance anyway - Control Engineering. Control Engineering. https://www.controleng.com/pid-spotlight-part-6-deadtime-how-to-boost-controller-performance-anyway/.
16. Wilkie, J.; Johnson, M.; Katebi, R. Poles, Zeros and System Stability. Control Engineering 2002, 242–276. https://doi.org/10.1007/978-1-4039-1457-6_10.
17. Gómez-Guerra, G.; Insuasti, S.; Camacho, O. Sliding Mode Control for Inverse Response Systems: A Trajectory Tracking Study. Proceedings of the 21st International Conference on Informatics in Control, Automation and Robotics 2024, 178–188. https://doi.org/10.5220/0013068300003822.
18. Miskon, M. T.; Fazalul Rahiman, M. H.; Taib, M. N.; Adnan, R. Comparative Assessment of PID Controller Tuning Methods for Coffee Roasting Process: Mohamad Taib Miskon, Mohd Hezri Fazalul Rahiman*, Mohd Nasir Taib Ramli Adnan. Journal of Tomography System & Sensors Application 2021, 4 (2), 74–81.
19. Halim, C. V.; Indriawati, K. Comparative Analysis of Cohen-Coon and Ziegler-Nichols Tuning Methods for Three-Phase Induction Motor with Speed Sensorless Control. Indonesian Journal of Electrical Engineering and Computer Science 2025, 39 (2), 885. https://doi.org/10.11591/ijeecs.v39.i2.pp885-895.
20. Eriksson, L. M.; Johansson, M. PID Controller Tuning Rules for Varying Time-Delay Systems. 2007 American Control Conference 2007, 619–625. https://doi.org/10.1109/acc.2007.4282655.
21. Balsa-Canto, E.; Banga, J. R. AMIGO, a Toolbox for Advanced Model Identification in Systems Biology Using Global Optimization. Bioinformatics 2011, 27 (16), 2311–2313. https://doi.org/10.1093/bioinformatics/btr370.
22. Diwakar, B.; Gokul Anandh, M.; Brindaa, R.; Brindaa, S. R.; Aravind, P. IMC Based Design of PI Controller for Real Time Pressure Process. IJIREEICE 2015, 3 (10), 12–15. https://doi.org/10.17148/ijireeice.2015.31003.
23. Chen, D.; Seborg, D. E. PI/PID Controller Design Based on Direct Synthesis and Disturbance Rejection. Industrial & Engineering Chemistry Research 2002, 41 (19), 4807–4822. https://doi.org/10.1021/ie010756m.
24. Sulaiman, S. F.; Rahmat, M. F.; Faudzi, A. 'Athif M.; Osman, K. Disturbance Rejection Using Model Predictive Control for Pneumatic Actuator System. 2016 IEEE 12th International Colloquium on Signal Processing & Its Applications (CSPA) 2016, 285–290. https://doi.org/10.1109/cspa.2016.7515847.
25. Arbogast, J. E.; Beauregard, B. M.; Cooper, D. J. Controller Tuning for Performance and Robust Stability. ResearchGate 2007, 1, 136–145.
26. Yazdan Bavafa-Toosi. Introduction to Linear Control Systems; Elsevier Academic Press: London, 2017.